RSC Applied Polymers

ROYAL SOCIETY OF CHEMISTRY

REVIEW

View Article Online
View Journal

Cite this: DOI: 10.1039/d5lp00101c

Harnessing near-infrared light for advanced 3D printing

Patrick Imrie *[a,b] and Jianyong Jin *[a,b]

Received 8th April 2025,
Accepted 27th May 2025

DOI: 10.1039/d5lp00101c

rsc.li/rscapplpolym

Light drives the curing process in many 3D printing strategies. To broaden the horizons of 3D printing, there is an ongoing push toward longer wavelengths for more effective, gentle, and precise layer photocuring of materials containing fillers or biological substances. Harvesting near-infrared (NIR) light (750–2500 nm) is at the forefront of this endeavour. Multiphoton lithography makes use of infrared light and is an established 3D printing technology, but it does require femtosecond pulse lasers. On the other hand, affordable NIR light sources can be used to 3D print objects with high precision, cytocompatibility, greater functionality, and from a wide range of polymers, but their implementation is not straightforward. In this review, recent studies are presented that advance the field of 3D printing with NIR light. Several cutting-edge technologies are identified, including support-free direct-ink-writing, *in vivo* bioprinting, and volumetric multimaterial modification, with a final perspective offered on volumetric projection printing toward high-throughput production.

1 Introduction

3D printing with light has been highly successful.[1] Vat photopolymerization (VP) 3D printing techniques, such as digital light processing (DLP) and stereolithography (SLA), work by irradiating liquid monomeric resin with light patterns to cure it in a layer-by-layer fashion.[2] The spatiotemporal control over the incident light gives VP 3D printing its excellent print fidelity. In

[a]*School of Chemical Sciences, The University of Auckland, Auckland 1010, New Zealand. E-mail: pimr761@aucklanduni.ac.nz*
[b]*Dodd-Walls Centre for Photonic and Quantum Technologies, Dunedin 9054, New Zealand. E-mail: j.jin@auckland.ac.nz*

Patrick Imrie

Patrick Imrie was born in Wellington, New Zealand. He completed his B.Sc. in Physics and Chemistry at the University of Auckland in 2019. He is currently pursuing a Ph.D. in Chemistry under the guidance of Dr Jianyong Jin and is a recipient of the University of Auckland Doctoral Scholarship. His research centers on advancing 3D and 4D printing technologies using RAFT and near-infrared polymerization mechanisms. Additionally, Patrick serves as a chemistry teaching assistant at the university and has a keen interest in Christian apologetics.

Jianyong Jin

Jianyong Jin is an associate professor in the School of Chemical Sciences at the University of Auckland. He received his B.Eng. in polymer materials engineering from Dalian University of Technology, his M.Sc. in macromolecular science from Fudan University, and his Ph.D. in organic synthesis and polymer chemistry from Clemson University, South Carolina. His academic research interests include microporous membranes for gas separation, biodegradable antimicrobial polymers, specialty polymers for laser micromachining, polymers for photonics and microelectronics, 3D printing via RAFT polymerization, "living" polymer networks, hydrogel, 4D printing, and multimaterial 3D printing.

addition to VP 3D printing, some multimaterial extrusion 3D printing techniques such as direct-ink-writing (DIW) use LEDs to cure ink after deposition, expanding the range of material that can be photocured.[3] In the majority of cases, the photocuring process in 3D printing is driven by short-wavelength light, usually between 365 to 460 nm. While high-energy light ensures rapid curing rates, several shortcomings have been noted by 3D printing researchers. These include high scattering, poor penetration depth, and overcuring problems.

To mitigate these issues, researchers have turned their attention to 3D printing with blue, green, and red light.[4–8] For example, our group and others have employed controlled radical polymerization mechanisms such as photo electron/energy transfer reversible addition–fragmentation chain transfer (PET-RAFT) polymerization for curing resins with blue, green, and red light DLP 3D printers.[9–13] In another example, Page's group used various photoredox catalysts alongside donor and acceptor co-initiators for rapid high-resolution DLP and liquid crystal display 3D printing with blue, green, and red light.[14,15] Shin *et al.* used a similar co-initiation system for rapid (8 s/layer) DLP 3D printing of clear resins with 620 nm light.[16]

To push the envelope of 3D printing, near-infrared (NIR) light (750–2500 nm) is used for photocuring in place of UV and visible light. NIR light has superbly low scattering and excellent penetration depth, especially in aqueous and biological systems.[17] This has led to the creation of some exceptional NIR 3D printing technologies. In fact, 3D printing with NIR light is not a new idea. Multiphoton lithography (MPL) is an established VP 3D printing technology that uses a femtosecond laser (usually 780–800 nm) to cure resin at the focal point.[18,19] The high intensity of the femtosecond laser ($\sim 10^{12}$ W cm^{-2}) grants the simultaneous absorption of multiple photons whose combined energies induce photopolymerization.[20,21] While MPL offers unprecedented print resolution (sub 100 nm), it is impractical for fabricating objects beyond the centimeter scale. This, combined with the high price of femtosecond lasers, limits the wide-scale adoption of MPL 3D printing. On the other hand, continuous-wave NIR lasers and LEDs are relatively inexpensive, versatile, and consistently emit light. NIR light is commonly used as a stimulus to induce shape transformations in the realm of 4D printing.[22–28] However, using it to photocure resins and inks during the 3D printing process is an emerging area of research, and its low energy requires the use of clever techniques.

In this review, the use of NIR light for 3D printing is examined. The first section details the benefits of using NIR light, including greater versatility and enhanced printing resolution. The second section examines the various NIR photocuring mechanims for 3D printing: upconversion materials (UCMs), photothermal conversion, type II photopolymerization, RAFT photopolymerization, and triplet–triplet annihilation (TTA). The third section looks at advanced 3D printing technologies enabled by NIR light: support-free direct-ink-writing, *in vivo* bioprinting, and volumetric multimaterial modification, with a final perspective offered on volumetric projection for high-throughput printing.

2 Benefits of NIR light in 3D printing

The most important benefit of NIR light is its penetration depth through a host of different materials. For example, NIR light penetrates approximately 10 times deeper into polystyrene latex than blue light, and approximately 100 times deeper than UV light.[29] This distinguishing feature is what makes state-of-the-art NIR 3D printing technologies possible (*e.g.*, support-free printing, *in vivo* bioprinting, volumetric printing, *etc.*). In VP 3D printing, NIR light attenuates more gradually, resulting in more evenly cured layers.[30,31] The layer thickness can also be enlarged beyond what is possible with shorter wavelengths. This means that larger objects can be printed more rapidly.

On account of its greater penetration depth, NIR light more effectively cures composite materials containing dispersed materials.[32] This is a big advantage for NIR 3D printing that expands the library of materials that can be 3D printed. Many polymeric composites contain ceramic particles for reinforcement, and the ability to 3D print these stiff and high-density materials is a significant step forward. Increasing the solid content in inks enhances their viscosity, which can be advantageous for NIR 3D printing.[33] This increased viscosity helps the inks maintain their shape better in their uncured state, though it may necessitate higher extrusion pressures. Additionally, higher viscosity resins are beneficial for freeform

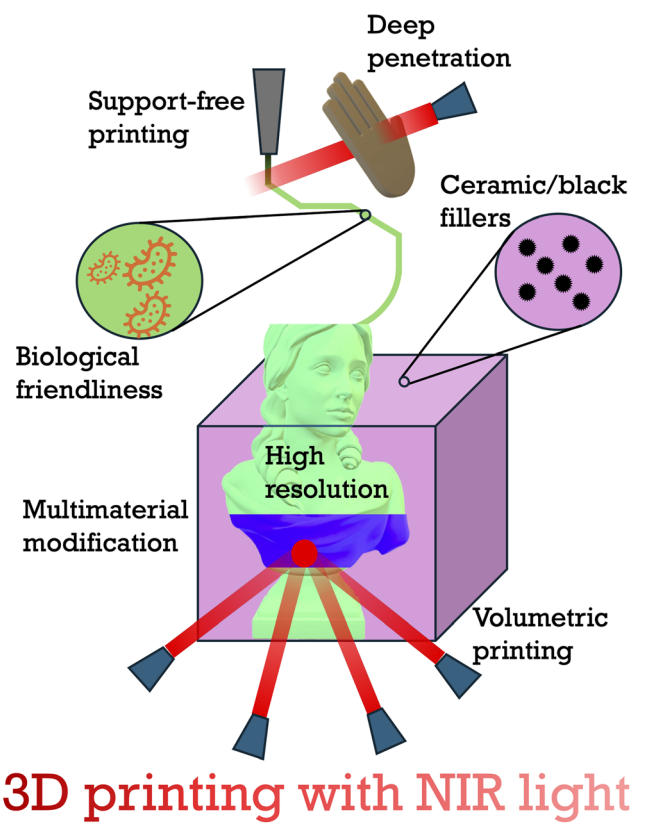

Fig. 1 Illustration highlighting the many unique benefits of 3D printing with NIR light.

Table 1 Summary of NIR light sources employed in various 3D printing systems, including their specific wavelengths, manufacturer and model numbers where appropriate

Manufacturer	Model	Country	Wavelength (nm)	Ref.
Changchun New Industries Optoelectronics Technology	FC-W-980H-50W	China	980	Liu *et al.*,[33,35,41–46] Chen *et al.*[47]
Changchun New Industries Optoelectronics Technology	MDL-H-808-5W	China	808	He *et al.*[34]
Shenzhen Fulei Technology		China	980	Zhang *et al.*[48]
Shenzhen Lamplic	UVEC-60X20	China	820	He *et al.*[34]
Innolume	LD-1064-UM-6W	Germany	1064	Porter *et al.*[49]
ATC – Semiconductor Devices		Russia	975	Rocheva *et al.*[50]
OdicForce Lasers	OFL371	UK	980	Zhakeyev *et al.*[51–54]
Thorlabs	BL976-PAG900	USA	976	Zhang *et al.*[55]
Luminus Devices	CBM-90-IRD	USA	869	Stevens *et al.*[56]
Opto Engine LLC	MDL-H-808	USA	808	Lee *et al.*[57]
Hyrel International	LA5-808	USA	808	Kam *et al.*[58]

volumetric printing, as the surrounding uncured resin can effectively serve as a support bath for the cured object.

Another area where NIR light proves useful is in curing composites with colored fillers that are challenging to 3D print using UV light. Black objects, in particular, are difficult due to their opacity to visible wavelengths. However, this issue can be overcome with NIR light.[34,35] Particle-polymer composites (PPCs) are also ubiquitous smart materials in the realm of 4D printing, and using NIR light may allow researchers to 4D print PPCs with higher particle loadings for more dramatic and responsive transformations.[22,25] In inks containing sensitive functional groups, using low-energy NIR light may prevent overcuring, which is when excessive UV light exposure leads to unwanted photolysis. For example, chain-transfer agents dispersed in "living" inks and resins are prone to photolysis with UV light which may affect their post-printing growth abilities.[36] Moreover, NIR-absorbing inks may offer better bench stability, being less susceptible to premature curing from ambient light.

In conjunction with more effective curing, NIR light may also promote better print resolution. Print resolution refers to the size limit of small features that can be crafted; in short, the smaller the features, the better the resolution. In extrusion-based 3D printers, this is mostly dependent upon nozzle size, extrusion pressure, and drag velocity. In VP 3D printers, this is directly related to the size of the voxels that make up the entire 3D object, which is dependent upon layer height (*i.e.*, how much the build-plate retracts for each layer), laser focal point/projector pixel size, and scattering of the incident light. Since VP 3D printers mostly work by directing the incident light vertically onto the resin, any scattering (*i.e.*, trajectory deviation) will necessarily worsen resolution in the horizontal plane. While photoabsorbers can be added to 3D printing resins to enhance edge sharpness, they are not always desirable since they often act as dyes that alter the color. According to Rayleigh's theory, the scattering of light is inversely proportional to its wavelength to the 4^{th} power.[37] Thus, shifting to longer wavelengths for VP 3D printing may vastly improve printing resolution.

NIR light also lends itself well to the field of bioprinting, which is 3D printing with biomedical application. DIW is often used to extrude cell-laden bioinks with the ambitious goal of replicating native tissue structures.[25] However, it is well known that UV light is damaging to cells; in fact, even excessive blue light (400–450 nm) can harm retinal cells.[38] Fortunately, light between 650 and 950 nm is used in many medical applications, including those involving photopolymerization, owing to its low absorption by water and tissue.[39,40] There is considerable interest in exploiting this therapeutic window to cure cell-laden bioinks with NIR light. Moreover, switching to NIR light is safer for the operator. Fig. 1 illustrates some of the advantages of NIR 3D printing, while Table 1 lists NIR light sources used for 3D printing.

3 NIR photocuring mechanisms

3.1 NIR upconversion materials

The most common method for utilizing NIR light in 3D printing involves lanthanide-doped UCMs.[59–61] Typically, UCMs have three important components: sensitizers, acceptors, and host inorganic lattice.[62] The sensitizers are lanthanide ions (typically Yb^{3+}) that absorb NIR photons. This energy is passed to other lanthanide ions, the acceptors (typically Tm^{3+}), and a series of energy transfers results in the emission of a high-frequency photon. The low-phonon-energy host lattice incorporates these ions into a crystal structure that helps to facilitate their interaction. The fluoresced high-frequency light is then absorbed by photoinitiators to instigate polymerization. Oftentimes, core/shell variants are synthesized by researchers for improved print precision. The added shell component (typically $NaYF_4$) protects the core component (typically $NaYF_4$:Yb^{3+},Tm^{3+}) from quenching by the surrounding environment. This greatly enhances its luminescence efficiency, allowing NIR light with lower intensity to be used for UCM-assisted photopolymerization.

The first genuine case of using UCMs for NIR stereolithography comes from Méndez-Ramos *et al.*[63] Organic resins con-

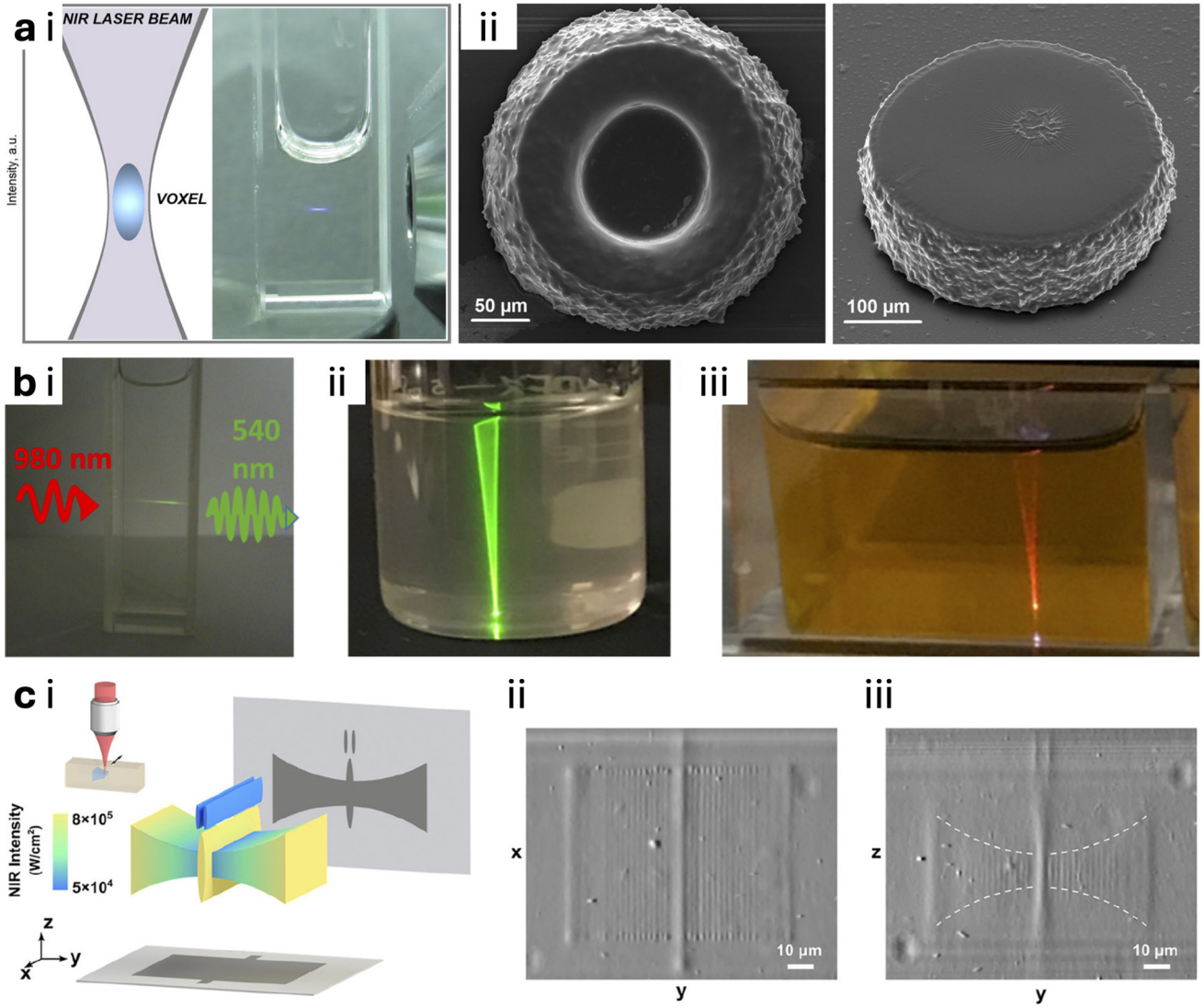

Fig. 2 (a) (i) Luminescent voxel formation in 10 mm × 10 mm cuvette containing light-sensitive resin impregnated with UCMs under continuous-wave NIR light illumination at 15 W cm^{-2} intensity. (ii) Scanning electron microscope images of 3D polymer microstructures obtained by NIR-light-activated photopolymerization in a thin layer. Reproduced with permission. Copyright 2018 Springer Nature.[50] (b) (i) Illustration of green light upconversion. Resin formulation: (ii) without; (iii) with 0.05 wt% Eosin Y and 2.5 wt% triethanolamine upon excitation with a 980 nm laser. Reproduced with permission. Copyright 2022 MDPI.[51] (c) Fabrication of a butterfly of tunable feature sizes with UCM-assisted multi-photon printing. (i) Butterfly model and its projections in two orthogonal directions. Differential phase contrast images of *xy*-plane (ii) and *yz*-plane (iii) show the scanning range and the feature size, respectively. Reproduced with permission. Copyright 2022 De Gruyter.[55]

taining poly(ethylene glycol) diacrylate (PEGDA), Irgacure-819 photoinitiator, and Tm^{3+}-doped K_2YbF_5 microcrystals were 3D printed into solid letter shapes. The setup used a commercial 980 nm laser which operated at low power (300 mW), highlighting the substantial improvement in efficiency over MPL. Thereafter, Yan *et al.* prepared core/shell β-$NaYF_4$:Yb^{3+},Tm^{3+}/$NaYF_4$ microparticles at different hydrothermal temperatures and with different Tm^{3+} concentrations.[64] These UCMs were included at different concentrations in resins containing trimethylolpropane triacrylate and photoinitiator 784. Through careful balancing of variables and using a 975 nm laser, stereolithographic 3D printing of letters was performed with an impressive maximum curing depth (*i.e.*, layer thickness) of 41 mm and a minimum curing cross-section diameter (*i.e.*, horizontal print resolution) of 0.22 mm.

An important characteristic of UCMs is their peculiar emission response to NIR excitation. UCMs initially absorb a photon to reach an intermediate state, and the absorption of additional photons excites them to an emissive state.[65] At first, the emission intensity increases quadratically with the incident NIR intensity, but beyond a certain crossover point, this relationship becomes linear. This emission intensity dependence is exploited in volumetric 3D printing, enabling selective voxel curing anywhere within the resin volume. By precisely

adjusting the power and optical focus of the NIR laser, researchers can ensure that the threshold intensity for photopolymerization is achieved exactly at the focal point. Volumetric printing is compatible with high-viscosity resins and allows the creation of complex structures without additional support.[66]

In one example, Rocheva *et al.* used core/shell β-$NaYF_4$:Yb^{3+},Tm^{3+}/$NaYF_4$ nanoparticles in their resin formulations that also contained acrylates and Irgacure 369.[50] A 975 nm semiconductor laser was focussed into a voxel with moderate intensity (7 W cm^{-2}), continually scanned in the horizontal plane (0.2 mm s^{-1}), and vertically displaced 10 μm to begin each new layer. This allowed for 3D printing in the resin volume at the micrometer scale, as shown in Fig. 2a. Following this, Liang *et al.* used a 980 nm laser to photocure resins containing $NaYF_4$:Yb^{3+},Tm^{3+} microcrystals, PEGDA, and Darocur TPO photoinitiator.[67] By focussing the laser (20–64 W cm^{-2}) with a convex lens, the group found they could selectively crosslink resin 16 mm below the surface. In 2022, Zhakeyev and Jose Marques-Hueso mixed NaYF:Yb^{3+},Er^{3+} UCM microparticles alongside sensitizer (Eosin Y) and co-initiator (triethanolamine) in clear commercial resin.[51] The UCMs converted 980 nm laser light from a custom-made 3D printer into green light (540 nm) to cure the resin at the focal point through photo electron/energy transfer (PET) between Eosin Y and triethanolamine, seen in Fig. 2b. Using this benign photocuring system is a step toward cell-friendly volumetric bioprinting.

The shape and size of the fluorescence volume of UCMs, and consequently the photocuring voxel, depend on the intensity of the incident NIR light.[68] This was demonstrated by Zhang *et al.*, who used core/shell $NaYF_4$:Yb^{3+},Tm^{3+}/$NaYF_4$ nanoparticles coated with lithium phenyl-2,4,6-trimethylbenzoylphosphinate (LAP) photoinitiator for superb initiation efficiency in hydrogel resins based on gelatin methacryloyl (GelMA).[55] The group modulated the intensity of a 976 nm laser from 7.7×10^4 to 1.1×10^6 W cm^{-2}, which caused an increase in transverse voxel size from 1.3 to 2.8 μm and an increase in axial size from 7.7 to 59 μm, without affecting degree of hydrogel polymerization. As shown in Fig. 2c, the intensity was modulated during 3D printing to form features of different sizes and create a microscale butterfly in 1 hour, which was five times faster than the estimated printing time at the minimum feature size. The body and antennae of the butterfly were also printed with a larger laser scanning range (80 μm up from 60 μm) that resulted in higher contrast in the lateral direction.

3.2 NIR photothermal conversion

The second most popular method for 3D printing with NIR light is photothermal polymerization. The mechanism is similar to that of UCM-assisted photopolymerization, where NIR light is converted into a more useful form of energy to be harnessed by the initiator. Instead of a photoinitiator, a thermal initiator is used, necessitating the presence of photothermal converter particles such as gold nanorods and carbon nanotubes. These photothermal converters absorb NIR photons and convert their energy into vibrations, producing heat.

Thermal polymerization is used in the additive manufacturing of silicone elastomers that possess mechanical properties superior to those of photopolymerizable acrylate-based resins.[57] However, applying thermal curing methods in the post-printing stage leaves time for the pre-crosslinked silicone to warp under its own weight, greatly affecting shape fidelity.[69] To address this, *in situ* photothermal curing is employed for 3D printing. It is necessary to use NIR light to drive the *in situ* photothermal curing process because of its high penetration ability that allows for homogeneous and complete polymerization of the product. In one example, Porter *et al.* used a 1064 nm laser to photothermally cure medical-grade silicone immediately upon extrusion.[49] The silicone contained carbon-based black dye to increase NIR absorbance and heating, and extrusion and laser parameters were tuned to achieve prime stiffness in the final products.

In a remarkable effort, Lee *et al.* developed a new additive manufacturing technology called heating at a patterned photothermal interface (HAPPI).[57,70] The technology works in a manner similar to stereolithography: a laser (808 nm) with programmable *x*–*y* movements points upwards at a resin vat, above which is a build plate that moves in the *z* direction. The crucial difference is that the NIR laser is used to heat the bottom of the resin vat made of black polytetrafluoroethylene (*i.e.*, the photothermal plate), and this heat is then transferred to the resin material directly above the point of laser contact, leading to localized thermal crosslinking at above 120 °C, as shown in Fig. 3a. HAPPI is used to 3D print thermosets that would otherwise not be compatible with stereolithography-type methods. The group achieved rapid layer curing (within 5 s) of unmodified commercial polydimethylsiloxane resin (Sylgard 184) and 3D printed overhanging objects such as a gyroid and skull cap.

Besides its compatibility with silicone, hydrogel 3D printing *via* NIR photothermal polymerization may be more cost-effective than 3D printing *via* UV/violet photopolymerization. This is because it does not require water-soluble photoinitiators, which tend to be scarce and expensive. Magdassi's group used a low-cost thermal initiator (sodium persulfate (SPS)) alongside a very low concentration of gold nanorods in aqueous hydrogel precursor solutions containing monomer (2-hydroxyethyl acrylate (HEA)) and crosslinker (PEGDA).[58] Gold nanorods function as photothermal converters; NIR light instigates the longitudinal surface plasmon resonance effect (electron oscillations parallel to the nanorods) that leads to localized temperature increase (around 90 °C). Using a stereolithography 3D printer equipped with an 808 nm laser (explained schematically in Fig. 3b), a honeycomb object was fabricated from this resin that did not contain any photointiator. Following this, the group instead used carbon nanotubes as photothermal converters in hydrogel precursor resins that also contained opaque black ink.[71] Stereolithography 3D printing (808 nm) of black domes, cubes, and pyramids was achieved with large layer thicknesses (0.7 mm).

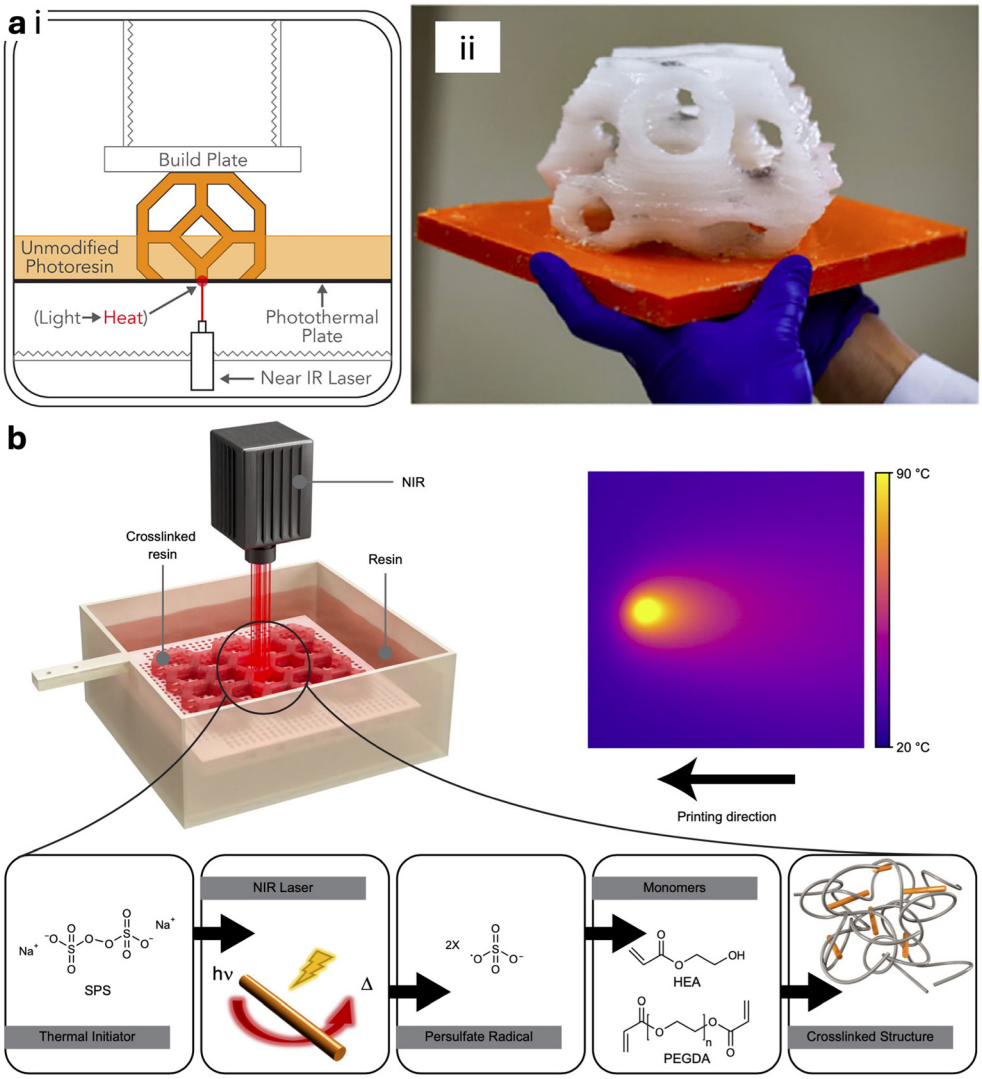

Fig. 3 (a) (i) Schematic of HAPPI additive manufacturing. Light is converted to heat at the photothermal plate, which induces thermal polymerization of the unmodified photoresin in contact with the plate. Reproduced with permission. Copyright 2023 Elsevier.[70] (ii) Complex 3D printed Sylgard 184 made *via* HAPPI additive manufacturing. Reproduced with permission. Copyright 2023 American Chemical Society.[57] (b) Scheme of NIR-induced stereolithography along with real-time temperature measurement *via* infrared camera. Below: structures and reactions in NIR-induced stereolithography. Reproduced with permission. Copyright 2024 Springer Nature.[58]

3.3 NIR type II photopolymerization

The two photocuring mechanisms discussed earlier both involve type I polymerization. In this process, NIR light is first converted into a more useful form of energy (*i.e.*, high-frequency light or heat), which is absorbed by photoinitiators or thermal initiators. In contrast, type II photopolymerization directly uses NIR light without conversion. Here, an NIR-absorbing sensitizer, often a cyanine, is excited by NIR light and undergoes the PET process to an acceptor co-initiator. This co-initiator, typically a diphenyliodonium salt (DPI), generates radicals to initiate polymerization.[72,73] Type II photopolymerization, which uses mild intensities, is increasingly being adopted for NIR 3D printing. Chemical structures of NIR-responsive photoredox components used or suggested for use are shown in Fig. 4.

Page's research group achieved rapid and high-resolution DLP 3D printing using low-intensity NIR light through a type II photocuring mechanism involving a cyanine photosensitizer (H-Nu 815) and a DPI acceptor.[56,74] An additional component, a borate salt co-initiator (borate V), also generated radicals by acting as an electron donor to the cyanine during the catalytic cycle. Layers of resin containing the photoredox components, 1,6-hexanediol diacrylate (HDDA) and pentaerythritol tetrakis(3-mercaptopropionate) were photocured in under 60 seconds using a DLP printer equipped with an 850 nm LED (4.6 mW cm^{-2}). The resulting structures demonstrated higher resolution, with features under 300 μm, compared to those printed with 405 nm light using the standard type I photopolymerization mechanism with bisacylphosphine oxide as the photoinitiator. Very recently, He *et al.* achieved stereolithographic NIR 3D print-

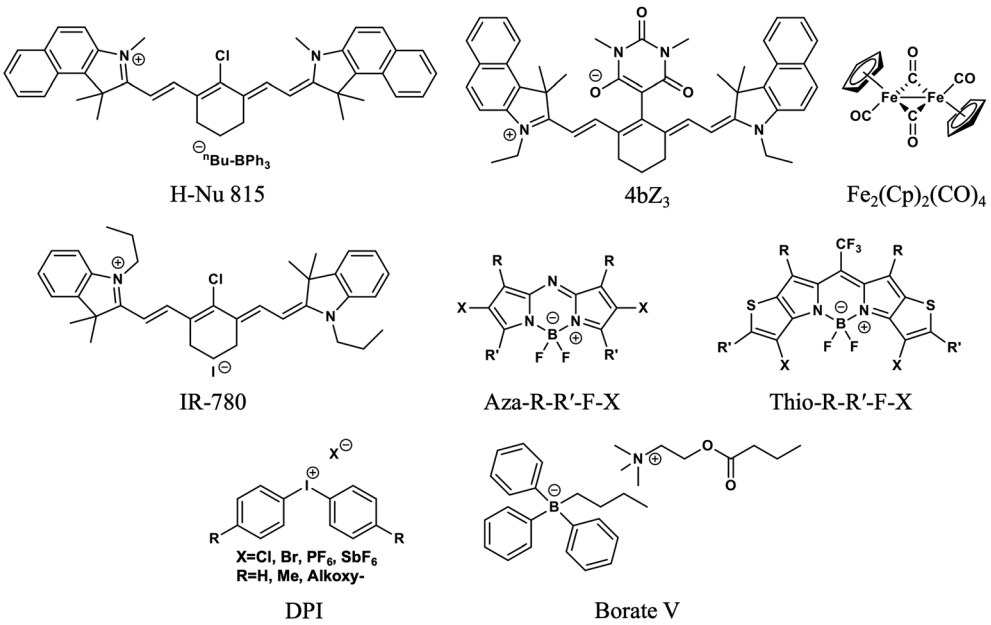

Fig. 4 Examples of photoredox components used or suggested for use in NIR-responsive 3D printing resins.

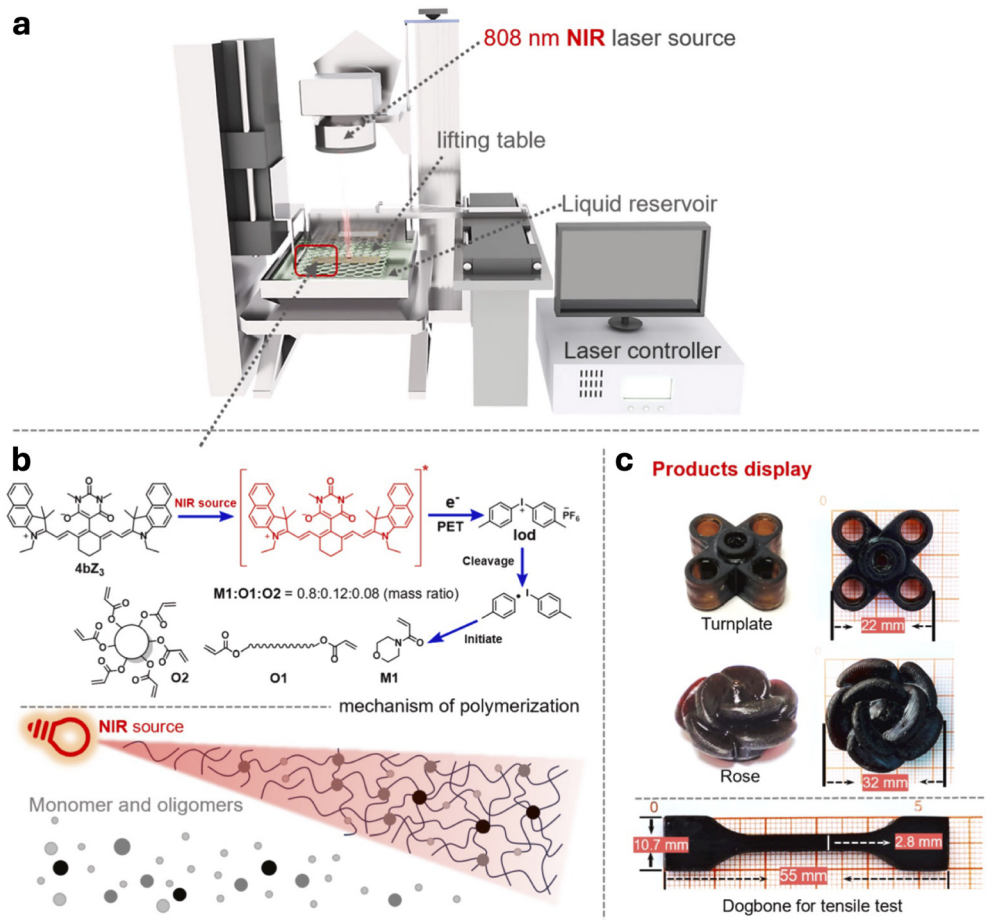

Fig. 5 (a) Physical structure of the NIR stereolithography 3D printing equipment. (b) Chemical mechanism of stereolithography 3D printing using 808 nm NIR light as the source. (c) Display of objects printed with a light intensity of 145 mW cm^{-2} and a scanning speed ranging from 200 to 280 mm s^{-1}. Reproduced with permission. Copyright 2025 Elsevier.[34]

ing *via* electron transfer between a cyanine ($4bZ_3$) and a DPI.[34] The 808 nm laser source (145–220 mW cm^{-2}) cured resins containing carbon black that functioned as both a black color filler and light absorber for improved printing precision (Fig. 5). The future of type II photopolymerization hinges on discovering more efficient NIR-absorbing photosensitizers,[75,76] with boron dipyrromethenes (BODIPYs, *e.g.*, Aza-R-R'-F-X and Thio-R-R'-F-X) emerging as promising contenders.[77,78]

3.4 NIR-RAFT photopolymerization

An established sector of 3D printing research is devoted to the marriage of controlled polymerization mechanisms with 3D printing technology.[3,22,79] Polymer networks prepared by controlled mechanisms such as reversible addition–fragmentation chain transfer (RAFT) polymerization have greater structural homogeneity,[80] gifting them enhanced mechanical and swelling capabilities useful in the fabrication of drug-delivery devices.[81] RAFT networks also have a "living" characteristic, making them capable of self-healing or growth effects in the post-printing stage, further enhancing their biological usefulness.[82] Furthermore, RAFT-based resins tend to have greater print resolution, useful for the construction of biomedical scaffolds with hierarchical porosity.[83] Therefore, there is a drive to make RAFT 3D printing more biologically friendly, particularly through the utilization of NIR-RAFT polymerization.[84]

In 2021, Zhao *et al.* presented radical-promoted cationic NIR-RAFT polymerization for stereolithography 3D printing (Fig. 6).[85] The polymerization mechanism proceeded by the NIR-driven decomposition of cyclopentadienyl iron dicarbonyl dimer ($Fe_2(Cp)_2(CO)_4$) followed by the reduction and decomposition of a DPI to produce radicals. These radicals reacted further with the DPI and diethylene glycol divinyl ether monomer to form cations for initiating cationic RAFT polymerization in the presence of a dithiocarbamate chain transfer agent. Using this approach, the group 3D printed single-layer letters up to 8 mm in thickness. As a final demonstration, post-production modification of the letters was carried out by restarting the RAFT process and inserting fluorescent monomers into the polymer chains.

While NIR light can cleave the weak iron-iron bond in $Fe_2(Cp)_2(CO)_4$ to generate metalloradicals, its effectiveness as a photoinitiator is limited by its low NIR absorption and potential toxicity.[86,87] Recently, the cyanine IR-780 was chosen to replace $Fe_2(Cp)_2(CO)_4$ in radical-promoted cationic NIR-RAFT polymerization.[88] This transition to a metal-free organic dye enhances biocompatibility, paving the way for applications in NIR-RAFT 3D bioprinting. The radicals for inducing cationic RAFT polymerization were generated *via* NIR-instigated PET between the excited cyanine and the DPI. Letters photocured with this mechanism demonstrated post-production welding capabilities, achieved by re-irradiating them with NIR light to restart the RAFT process and fuse the polymer chains together.

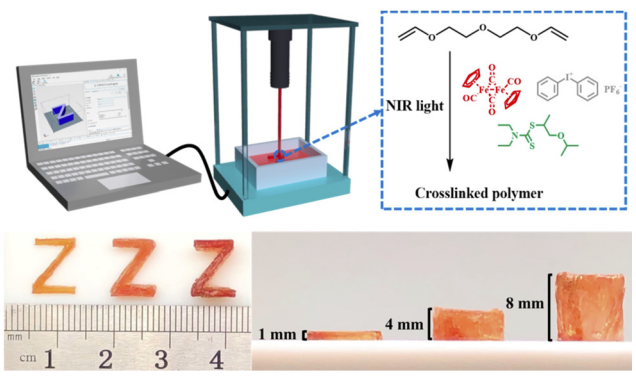

Fig. 6 RAFT stereolithography process under NIR light at 25 °C used to 3D print objects with different thicknesses. Reproduced with permission. Copyright 2021 American Chemical Society.[85]

3.5 NIR triplet–triplet annihilation possibilities

Triplet–triplet annihilation (TTA) is a highly efficient upconversion mechanism that enables 3D printing at significantly lower intensities compared to UCMs.[89] Mechanistically, TTA shares similarities with both UCMs and type II photopolymerization. This process involves two chromophores: a photosensitizer and an annihilator. The photosensitizer is excited by a low-energy photon and undergoes intersystem crossing to a triplet state. The energy is then transferred to a triplet annihilator. Two triplet annihilator molecules interact to produce a singlet excited state, which subsequently emits a high-energy photon. Like UCMs, TTA demonstrates a quadratic-to-linear emission dependence and can be used for volumetric printing with a focused laser.[90] Photosensitizers commonly used in type II photopolymerization, such as cyanines, could also be used in TTA processes if they can reach triplet excited states.

To date, TTA-based 3D printing has been successfully implemented using green and red light, but has not yet been achieved with NIR light.[91–96] For realistic printing speeds, a large anti-Stokes shift (~1 eV) is necessary so the emitted light can be absorbed by photoinitiators, facilitating radical polymerization. Lalevée's group accomplished free radical polymerization of acrylates *via* NIR-to-blue TTA upconversion.[97] They utilized metal-free cyanine photosensitizers (S2025 or S0507) which absorbed 785 nm light from a laser diode (2.5 W cm^{-2}) and transferred the triplet energy to a 2,5,8,11-tetra-*tert*-butylperylene annihilator, which emitted blue light (peak 500 nm). This light was absorbed by the photoinitiator Irgacure 784, with a maximum absorption at 470 nm. However, much of the polymerization was attributed to a competing photothermal effect, indicating that the photosensitizers were significantly quenched by the surrounding environment.

Indeed, TTA is highly susceptible to quenching as resin viscosity increases during curing, necessitating high concentrations of photosensitizers and annihilators.[98] Additionally, it faces the same oxygen intolerance issues that have historically affected Type II photopolymerization, as molecular oxygen in its triplet ground state rapidly reacts with photosensitizers and triplet-excited excitons. To protect against quenching and increase local concentration, Sanders *et al.* encapsulated a palladium(II)-porphyrin photosensitizer and anthracene-based annihilator within nanocapsules made from poly(ethylene glycol) chains on silica shells.[90] These nanocapsules were dispersed in organic-solvent-based resins containing Ivocerin photoinitiator. Volumetric print-

ing of a small boat (289 layers with 50 μm thickness) was achieved by focusing a 637 nm laser to initiate the red-to-blue TTA upconversion process and photoinitiation at the focal point. Recently, Peng *et al.* developed oxygen-resistant TTA nanoparticles for photobiocatalysis by incorporating a platinum(II) photosensitizer within an amphiphilic polymer.[99] These TTA nanoparticles exhibited NIR-to-blue upconversion with a quantum yield of 1.8%, surpassing the typical yield of UCMs, which is usually below 1%.[98] Their ability to disperse in water makes them promising for applications in 3D printing hydrogels.

4 Evolution and future directions of NIR 3D printing

4.1 Support-free direct-ink-writing

One of the most exciting additive manufacturing technologies currently in development is support-free DIW 3D printing.[100] Liu *et al.* have made large strides in support-free 3D printing through their use of NIR photocuring. In 2020, the group developed a photoink containing UCMs, titanocene photoinitiator, trifunctional monomer trimethylolpropane acrylate and difunctional monomer bisphenol A epoxy acrylate, that rapidly formed a crosslinked polymer network when irradiated with a 980 nm laser upon extrusion.[41] The *in situ* photocuring procedure resulted in much greater print fidelity than the normal post-printing curing protocol, as the extruded material had no time to relax and bulge outwards before solidifying. The use of highly penetrating NIR light meant extruded ink with a large diameter (4 mm) could be photocured, and the non-interference of NIR light with added dyes allowed the group to 3D print freestanding multicolor structures, as shown in Fig. 7a. In the same year, the group also showed how a similar NIR DIW strategy could be used to 3D print objects with highly absorbing white and black filler (titanium white and melanin, respectively) that are notoriously tricky to cure with UV and visible light.[35] Subsequently, NIR DIW 3D printing of polymeric cubes containing a high percentage (92%) of glass fibre was achieved by studying the filling aggregation-induced extinction mechanism, which revealed that NIR light extinction depends on both the characteristic size of the filler particles and the wavelength of the incident light.[43] The group also enhanced the print speed, resolution, and oxygen tolerance of photoinks for NIR DIW 3D printing by optimizing the composition of UCMs, photoinitiators, and co-initiators.[42]

In a breakthrough study published in 2023, Liu *et al.* achieved unsupported DIW 3D printing of a polymeric/ceramic slurry through laser photocuring (Fig. 7b).[33] Ceramic slurries are an attractive material for support-free DIW because of their high resultant stiffness after solidification. However, the high solid

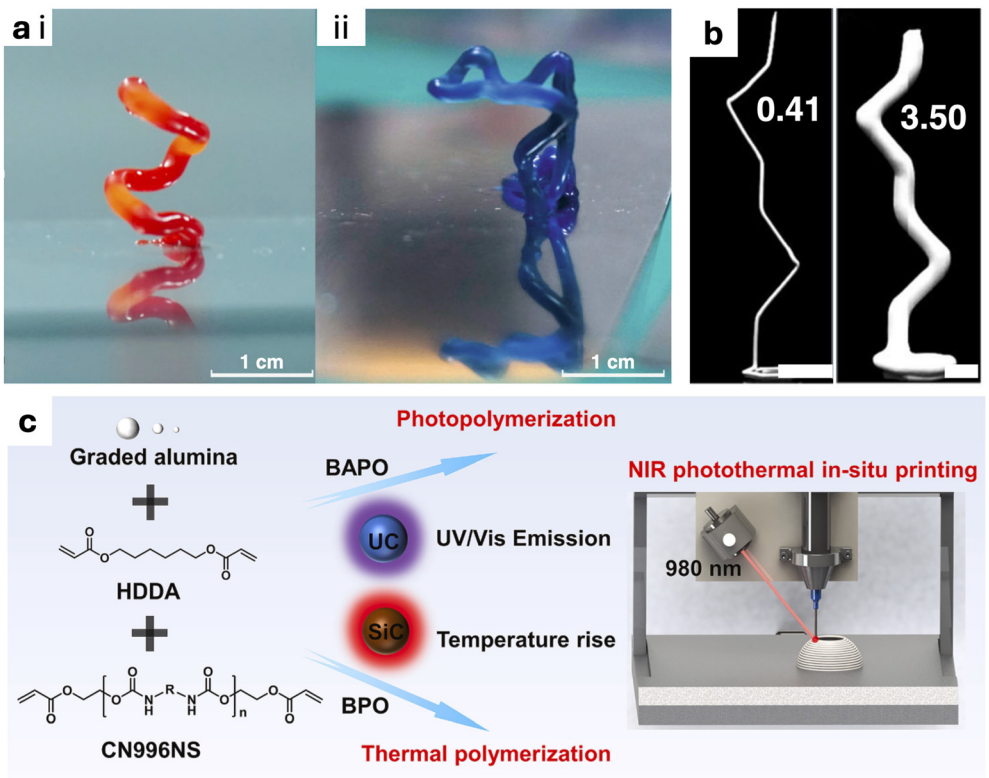

Fig. 7 (a) NIR-DIW-printed colored freestanding structures. (i) Freestanding spiral structure with red pigments. (ii) Freestanding M-shaped cantilever structure with blue pigments. Reproduced with permission. Copyright 2020 Springer Nature.[41] (b) Filaments with different size nozzles (0.41 and 3.50 mm) cured *in situ* with the assistance of NIR. The scale bars are equivalent to 5 mm. Reproduced with permission. Copyright 2023 Springer Nature.[33] (c) Schematic diagram of NIR photothermal synergistic assisted DIW printing. Reproduced with permission. Copyright 2023 Elsevier.[44]

content of ceramic slurries introduces additional light scattering, refractive indices and extinction coefficients, hampering curing efficiency with UV/visible light. To circumvent this, the group used a 980 nm laser setup that could rapidly photocure the ink containing UCMs, alumina ceramic powder, phenylbis(2,4,6-trimethylbenzoyl)phosphine oxide (BAPO) photoinitiator, difunctional polyurethane acrylate (CN996NS), and difunctional HDDA. Following this, the group improved the NIR-induced polymerization efficiency by incorporating photothermal converter (silicon carbide (SiC)) and thermal initiator (benzoyl peroxide (BPO)) in the printing ink (Fig. 7c).[44] The thermal initiator was activated by heat from both photothermal conversion and the upconversion process. This worked synergistically with the photoinitiator, resulting in improved curing depths and compatibility with high alumina content (90 wt%). This photothermal synergetic curing effect was also used to rapidly 3D print polymeric ink with enhanced mechanical properties and surface sharpness.[45] Most recently, the distance between UCMs and BAPO photoinitiator was reduced to accelerate NIR photocuring and augment 3D printing throughput.[46] This was achieved by electrostatically attaching to the UCMs metal–organic frameworks, within which were housed BAPO particles.

4.2 *In vivo* 3D bioprinting

3D bioprinting is the use of 3D printing technology for biomedical applications.[3] The ultimate end of 3D bioprinting is the production of a human organ for transplantation.[101] As noted by Wang, only by using living cells and biodegradable polymers can 3D bioprinting be used to permanently and totally restore failed organs.[102] Therefore, a key factor in the advancement of 3D bioprinting is the ability to deposit living cells viably contained within biodegradable material in order to

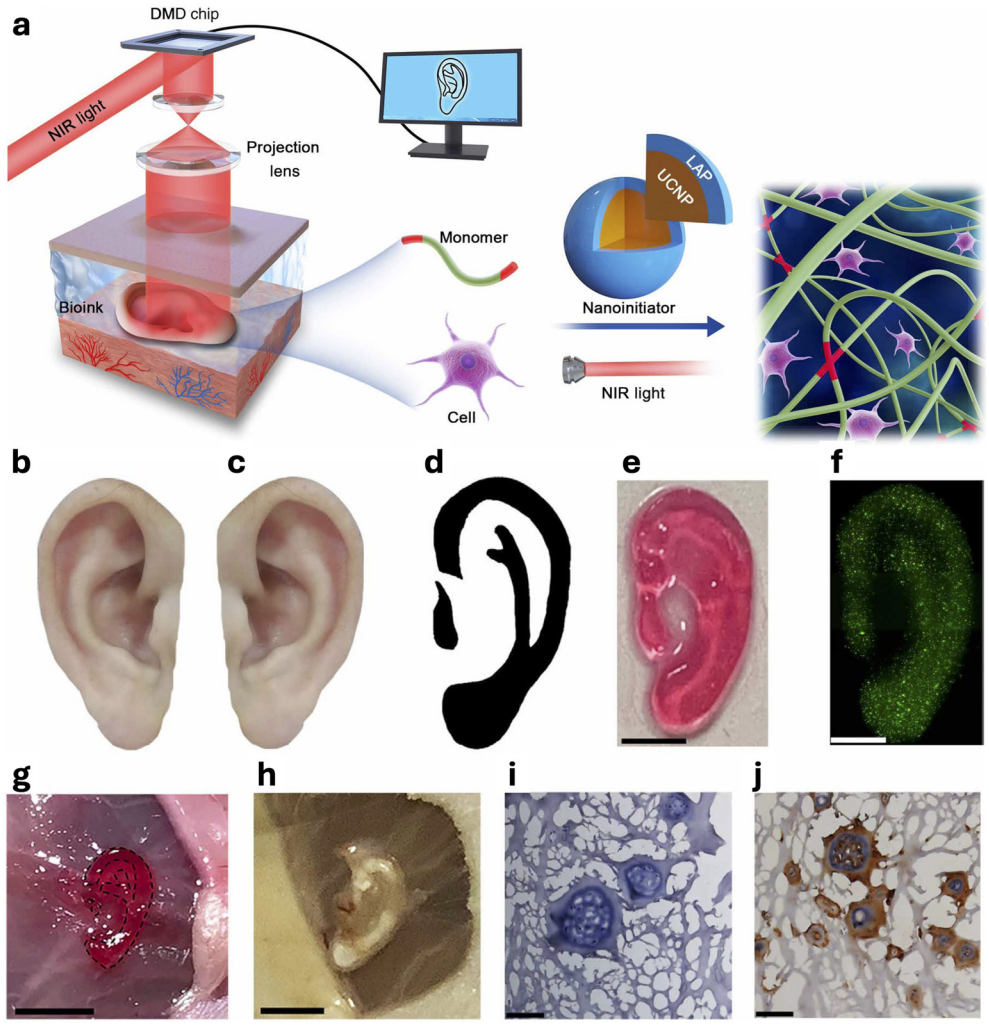

Fig. 8 (a) Schematic diagram of *in vivo* 3D bioprinting. (b–j) Noninvasive 3D bioprinting of ear-like tissue. (b) Representative image of the normal ear. (c) Mirror image of (b). (d) Optimized ear-outline image of (c). (e) Image of printed ear-like construct from the bioink covered over by skin. Scale bar, 2 mm. (f) The live/dead staining for ear constructs encapsulated with chondrocytes bioprinted from bioink covered by skin after culture for 7 days. Scale bar, 2 mm. (g) Noninvasive 3D bioprinting of ear-shaped construct *in vivo*. Scale bar, 5 mm. (h) Representative image of bioprinted ear-shaped construct at 1 month. Scale bar, 5 mm. (i) H&E and (j) collagen type II immunostaining of retrieved ear-shaped construct at 1 month. Scale bars, 50 μm. Photo credit: Yuwen Chen, State Key Laboratory of Biotherapy and Cancer Center. Reproduced with permission. Copyright 2020 American Association for the Advancement of Science.[47]

replicate human tissue. In the majority of cases, this involves mixing cells in hydrogel precursor solution/ink that is crosslinked with UV/violet light in a layer-by-layer fashion. However, high-frequency light is known to cause harm to living cells, necessitating the transition to longer NIR wavelengths.[103]

In addition to its biological benignity, a major selling point of NIR light is its ability to penetrate and drive photocuring reactions through tissue barriers. This attractive quality inspires research in the ambitious sector of *in vivo* 3D bioprinting, where fabrication of artificial organs is performed subcutaneously. In a groundbreaking effort from Chen *et al.*, a customized ear-like living construct was 3D printed *in vivo* inside a nude mouse (Fig. 8).[47] To achieve this, the group began by subcutaneously injecting a bioink consisting of chondrocytes, GelMA, and UCMs coated with LAP. Then, data from the CAD model of an ear were sent to a digital micromirror device (DMD), and the reflected 980 nm light patterns were focussed by an optical lens through the skin of the mouse to grow the ear in 20 seconds. The 3D printed ear gradually chondrified, proving the feasibility of using NIR light for *in vivo* organ 3D bioprinting.

The difficulty with *in vivo* 3D bioprinting is printing multiple layers, as there is no build plate to move construction in the vertical direction. To address this, Zhang *et al.* used a coordinate positioning system to move the focal point of a 980 nm laser in three dimensions, enabling the group to volumetrically bioprint scaffolds from bioink (GelMA, propylene, photoinitiator, UCMs) injected within fracture sites. The use of a NIR laser for subcutaneous photocuring of bioink containing UCMs has been demonstrated in other similar works from Karami *et al.* and Liu *et al.*, and will likely be the go-to method for *in vivo* 3D bioprinting of more complex anatomical replicates in future.[104,105] For safety reasons, it is important to note that the American National Standard for safe use of lasers sets the maximum permissible NIR intensity exposure to skin at 0.726 W cm^{-2}.[106]

4.3 Volumetric multimaterial modification

The ability to 3D print objects comprising multiple materials is perhaps the most important aspect of 3D printing advancement.[3] For multimaterial 3D printing to be viable, there

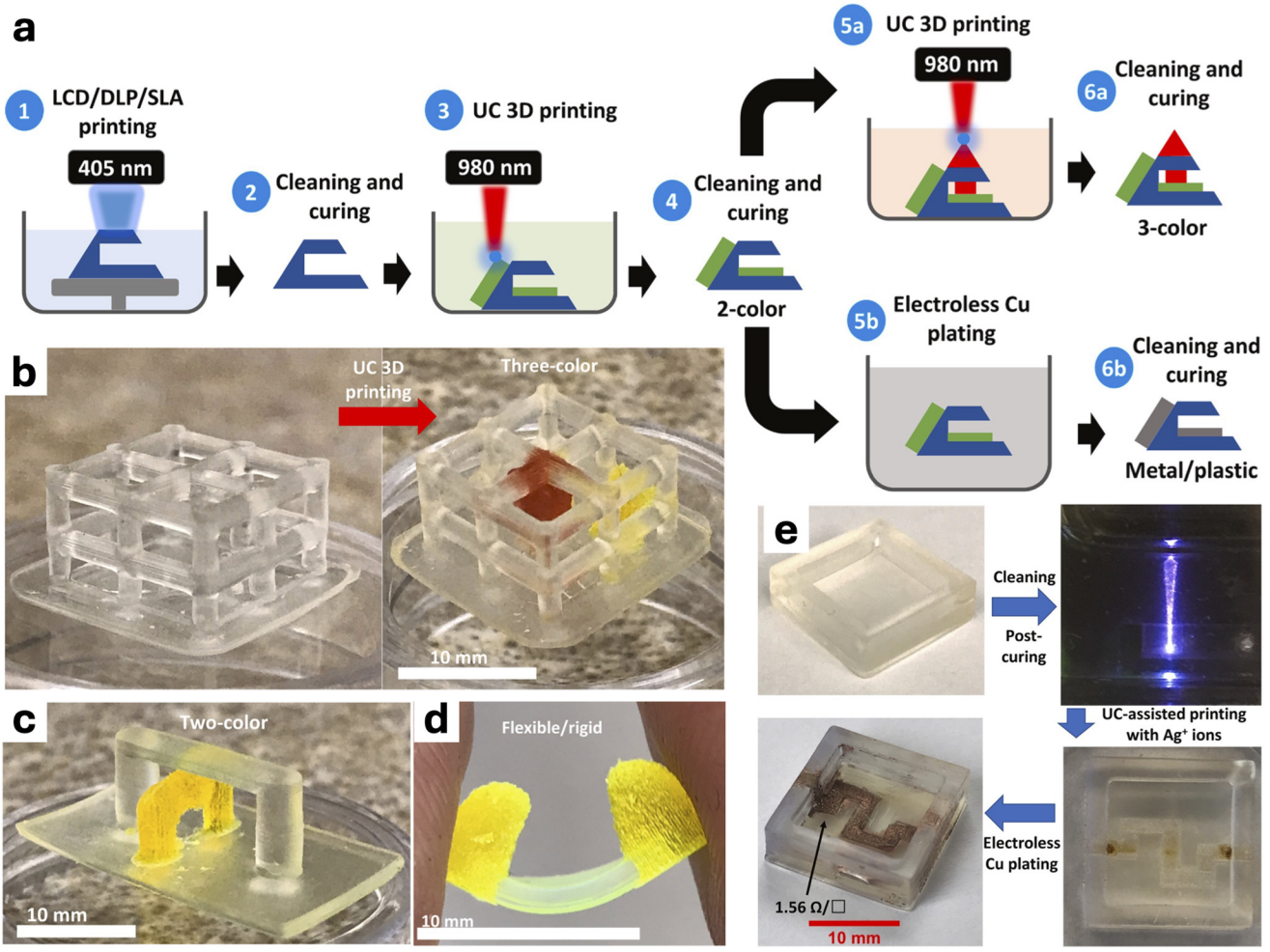

Fig. 9 (a) Schematic representation of the proposed upconversion-assisted multimaterial stereolithography process. (b) Three-color print. (c) Two-color "bridge under another bridge". (d) Flexible/rigid print. (e) Processes for stereolithography printing metal/dielectric objects *via* upconversion-assisted crosslinking and selective metallization. Reproduced with permission. Copyright 2023 Elsevier.[54]

should be an option to deposit new material anywhere within the object during fabrication. In an exciting series of publications from Zhakeyev *et al.*, NIR-induced crosslinking at the focal point was shown to be a potent tool for multimaterial modification.[52–54] After being 3D printed, polymeric parts were immersed in resin containing UCMs and dyes.[54] A 3D printer with a 980 nm laser was used to volumetrically cure the resin at depths of up to 5.8 cm.[52] Multicolor objects were created by sequential immersion of printed parts in vats with dyed resins, followed by selective irradiation on or within the objects, as shown in Fig. 9. Similarly, multimaterial objects with rigid/soft regions were created with acrylate/elastomer resins. This versatile multimaterial modification method can reduce waste by allowing changes in the 3D design to be applied directly to the previous physical iteration, thereby decreasing the number of prototypes needed. It also has potential to be used as a repair and restoration protocol for damaged 3D printed parts. The group also mixed silver ions alongside UCMs in clear commercial resin that worked synergistically to increase NIR-induced curing speed tenfold.[53] The silver ions doubled as seeding sites for electroless copper plating of the printed parts, forming a conductive path with a sheet resistance of 1.56 ± 0.24 Ω. This demonstrates the method's potential to create multimaterial electronic circuits.

4.4 Volumetric projection printing

A key player in the future of 3D printing is volumetric projection. Volumetric projection is a continuous VP method that could soon enable high-throughput manufacturing, potentially rivalling subtractive manufacturing on the factory line. Being a layer-less printing method, it pledges isotropic mechanical properties and zero chance of delamination. The two main forms of volumetric projection are tomographic and xolographic 3D printing. Tomographic 3D printing was invented in 2019 by researchers from California.[107] In tomographic 3D printing, a dynamic light pattern is projected through a rotating, clear, and cylindrical vat full of resin (Fig. 10a).[108] After a full 360 degree rotation, the cumulative light intensity from every angle overcomes the critical dose threshold, leading to a sol–gel transition in the resin and a solid 3D object. Xolographic 3D printing was invented a year later by a team from Germany.[109] In xolographic 3D printing, a thin light sheet (*xy*-plane) is projected through a resin and moved in the *z* direction, exciting photoinitiators from a dormant state to a latent state. At the same time, a dynamic light pattern is projected through the resin in the *z* direction, and wherever it intersects with the thin light sheet, it excites the latent photoinitiators and instigates curing (Fig. 10b).[110] Both tomographic and xolographic 3D printing are expected to undergo substantial improvements within a decade thanks to NIR light.

As both tomographic and xolographic 3D printers require deep penetration of UV/visible light, they are only compatible with resins that strongly transmit these wavelengths.[111] This narrows the range of material that can be printed. As discussed earlier, NIR has fantastic penetration depth through many different materials, so switching from UV/visible light to NIR

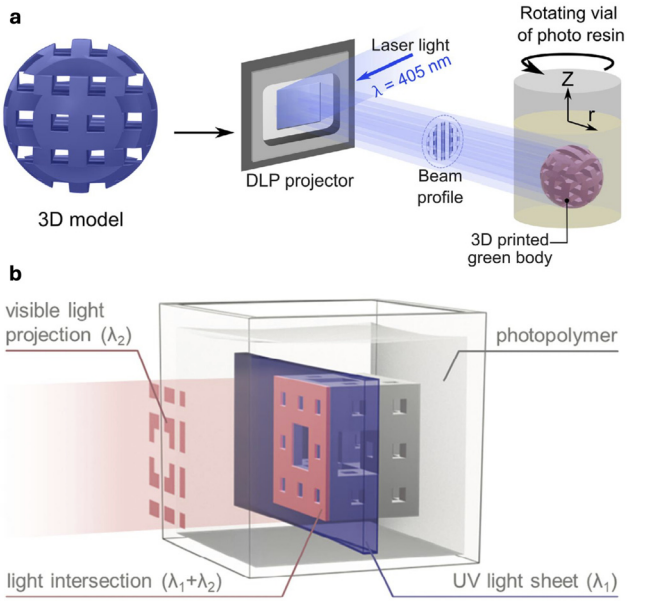

Fig. 10 Current state-of-the-art volumetric projection printing. (a) Tomographic 3D printing of a green body achieved by calculating a set of light patterns from the 3D model of the desired part which are projected onto a rotating vial filled with a photocurable resin. Reproduced with permission. Copyright 2022 John Wiley and Sons.[108] (b) Xolographic 3D printing achieved by moving a thin light sheet continuously through a photopolymer vat while an orthogonal light projection intersects (λ_1 + λ_2) to define the space coordinates for photopolymerization in the volume. Reproduced with permission. Copyright 2024 John Wiley and Sons.[110]

light could liberalize the content of compatible resins. Furthermore, the deeper penetration of the projected NIR images would allow for larger objects to be printed. A continuous flow of new resin into the vats could be used to volumetrically print large objects in the style of an assembly line, bringing the throughput of additive manufacturing up the level of subtractive manufacturing.[112] The long path through the resin gives projected light more opportunity to scatter, worsening the resolution of volumetric projection. Tomographic 3D printing resolution is particularly hampered by dose fluctuations through partially polymerized areas.[109] By switching to NIR light, the projected light would scatter less and hold its shape better through the resin. Thus, NIR volumetric projection would offer high resolution without sacrificing object size.

Tomographic 3D printing relies upon a nonlinear resin response to establish an intensity threshold for gelation.[109,113] This is typically achieved by exploiting oxygen in the resin for radical scavenging until a critical concentration is reached.[114] As discussed earlier, TTA is a nonlinear process and with the development of more efficient NIR-absorbing photosensitizers, deep tomographic 3D printing could become feasible.[90] The nonlinearity of NIR-absorbing UCMs makes them another potential option; however, their excitation lifetime—hundreds of microseconds—is insufficient for successive light projection.[115] A possible solution is to irradiate the cylindrical vat

from all angles with NIR patterns using a ring-shaped projector.

The high resolution of xolographic 3D printing results from the intersection of two different wavelength projections (375 and 550 nm) at the target voxel, functioning like an AND gate that cures only when both wavelengths are present. Switching to longer wavelengths for upscaled xolographic 3D printing may soon be possible. Zhu *et al.* demonstrated a dual-wavelength AND gate photopolymerization method with 721 and 532 nm light.[116] A solution containing a phthalocyanine complex functioned as a converging lens when irradiated with 721 nm light *via* a thermal lensing effect (TLE). A divergent 532 nm laser beam passed through the TLE solution and instigated TTA upconversion. When the 721 nm light was turned on, the TLE effect occurred in the solution, collimating the 532 nm laser beam and increasing the TTA upconversion emission intensity 6.7-fold, leading to rapid photopolymerization.

4.5 Challenges and future research

The primary challenge of NIR 3D printing is the inherently low energy of NIR light. Currently, UCMs are the standard for utilizing NIR light in 3D printing. Although UCMs operate at lower intensities than MPL, their required intensities are still quite high, necessitating focused lasers that can be impractical and slow down printing speeds. Our goal is to move beyond UCMs toward photocuring methods that work with low irradiation intensities (~10 mW cm^{-2}), employing techniques like type II photopolymerization, RAFT photopolymerization, and TTA upconversion. From a chemistry perspective, the key focus should be on developing NIR-absorbing photosensitizers for these methods, such as cyanines with enhanced NIR absorption and more efficient intersystem crossing. Additionally, incorporating thermal initiators in the resin or ink could further enhance curing effectiveness by utilizing excess heat generated through photothermal conversion.

The biomedical field presents the most promising application for NIR 3D printing. Support-free DIW and volumetric projection printing enable the creation of artificial organs without layers, significantly enhancing printing speed and potentially improving the durability of the organs. These methods can be executed without additional supporting structures, which often damage objects during post-production removal. Support-free DIW is excellent for producing hard objects with ceramics. The next step involves creating bone scaffolds using bioink containing GelMA, hydroxyapatite, chondrocytes, and osteocytes.[100] Tomographic volumetric projection printing is also effective for producing artificial soft organs, like the heart, from multiple materials, though current demonstrations are limited to the millimeter scale due to inadequate light penetration.[3,117] We recommend focusing on extending the operating wavelengths of tomographic printing rather than xolographic printing for NIR 3D bioprinting, as tomographic printing uses a single wavelength projected in all directions, avoiding any dimensional compromise. Lastly, we anticipate that *in vivo* 3D bioprinting, volumetric multimaterial modification, and "living" RAFT photopolymerization will converge into a comprehensive method for subcutaneous repair of artificial organs.

5 Conclusion

While harnessing NIR light for 3D printing presents challenges due to its low photon energy, its advantages—such as biological friendliness, low scattering, and remarkable penetration depth through various materials—make it a compelling choice. To exploit NIR light, it is often converted at the focal point into more useful forms of energy, either by upconverting to higher-frequency light using UCMs or by converting to heat. Additionally, there is growing interest in using photosensitizers that efficiently absorb wavelengths beyond 780 nm, enabling 3D printing with low-intensity NIR LEDs (<5 mW cm^{-2}) *via* type II, RAFT, and TTA photocuring. The unique attributes of NIR light have facilitated the development of advanced 3D printing techniques, including support-free DIW, *in vivo* 3D bioprinting, and volumetric multimaterial modification. Moreover, NIR light is poised to transform volumetric projection into a high-throughput production line. The pioneering studies examined in this review point to a bright future for NIR 3D printing that is almost visible.

Data availability

No primary research results, software or code have been included and no new data were generated or analysed as part of this review.

Conflicts of interest

There are no conflicts to declare.

Acknowledgements

J. J. would like to thank the New Zealand Ministry of Business, Innovation and Employment (MBIE) Endeavour Fund for funding the Advanced Laser Microfabrication for NZ Industries Research Programme (Grant UOAX-1701). P. I. is supported by the University of Auckland Doctoral Scholarship.

References

1 A. Bagheri and J. Jin, Photopolymerization in 3D printing, *ACS Appl.Polym. Mater.*, 2019, **1**(4), 593–611.
2 C. Dileep, L. Jacob, R. Umer and H. Butt, Review of vat photopolymerization 3D printing of photonic devices, *Addit. Manuf.*, 2024, 104189.
3 P. Imrie and J. Jin, Multimaterial hydrogel 3D printing, *Macromol. Mater. Eng.*, 2024, **309**(2), 2300272.

4 S. Sakai, H. Kamei, T. Mori, T. Hotta, H. Ohi, M. Nakahata and M. Taya, Visible light-induced hydrogelation of an alginate derivative and application to stereolithographic bioprinting using a visible light projector and acid red, *Biomacromolecules*, 2018, **19**(2), 672–679.
5 Z. Zheng, D. Eglin, M. Alini, G. R. Richards, L. Qin and Y. Lai, Visible light-induced 3D bioprinting technologies and corresponding bioink materials for tissue engineering: a review, *Engineering*, 2021, **7**(7), 966–978.
6 Z. Wang, H. Kumar, Z. Tian, X. Jin, J. F. Holzman, F. Menard and K. Kim, Visible light photoinitiation of cell-adhesive gelatin methacryloyl hydrogels for stereolithography 3D bioprinting, *ACS Appl. Mater. Interfaces*, 2018, **10,(32)**, 26859–26869.
7 Y. Zhang, Y. Xu, A. Simon-Masseron and J. Lalevée, Radical photoinitiation with LEDs and applications in the 3D printing of composites, *Chem. Soc. Rev.*, 2021, **50**(6), 3824–3841.
8 N. Lopez-Larrea, A. Gallastegui, L. Lezama, M. Criado-Gonzalez, N. Casado and D. Mecerreyes, Fast Visible–Light 3D Printing of Conductive PEDOT: PSS Hydrogels, *Macromol. Rapid Commun.*, 2024, **45**(1), 2300229.
9 A. Bagheri, H. Ling, C. W. A. Bainbridge and J. Jin, Living polymer networks based on a RAFT cross-linker: toward 3D and 4D printing applications, *ACS Appl. Polym. Mater.*, 2021, **3**(6), 2921–2930.
10 A. Bagheri, C. W. A. Bainbridge, K. E. Engel, G. G. Qiao, J. Xu, C. Boyer and J. Jin, Oxygen tolerant PET-RAFT facilitated 3D printing of polymeric materials under visible LEDs, *ACS Appl. Polym. Mater.*, 2020, **2**(2), 782–790.
11 A. Bagheri, K. E. Engel, C. W. A. Bainbridge, J. Xu, C. Boyer and J. Jin, 3D printing of polymeric materials based on photo-RAFT polymerization, *Polym. Chem.*, 2020, **11**(3), 641–647.
12 C. W. A. Bainbridge, A. Wangsadijaya, N. Broderick and J. Jin, Living polymer networks prepared by controlled radical polymerization techniques, *Polym. Chem.*, 2022, **13**(11), 1484–1494.
13 A. Bagheri, C. Bainbridge and J. Jin, Visible light-induced transformation of polymer networks, *ACS Appl. Polym. Mater.*, 2019, **1**(7), 1896–1904.
14 L. M. Stevens, E. A. Recker, K. A. Zhou, V. G. Garcia, K. S. Mason, C. Tagnon, N. Abdelaziz and Z. A. Page, Counting all photons: efficient optimization of visible light 3D printing, *Adv. Mater. Technol.*, 2023, **8**(23), 2300052.
15 D. Ahn, L. M. Stevens, K. Zhou and Z. A. Page, Rapid high-resolution visible light 3D printing, *ACS Cent. Sci.*, 2020, **6**(9), 1555–1563.
16 S. Shin, Y. Kwon, C. Hwang, W. Jeon, Y. Yu, H. J. Paik, W. Lee, M. S. Kwon and D. Ahn, Visible–Light–Driven Rapid 3D Printing of Photoresponsive Resins for Optically Clear Multifunctional 3D Objects, *Adv. Mater.*, 2024, **36**(19), 2311917.
17 F. Qiu, J. Gong, G. Tong, S. Han, X. Zhuang and X. Zhu, Near–infrared Light–Induced Polymerizations: Mechanisms and Applications, *ChemPlusChem*, 2024, **89**(6), e202300782.
18 V. Harinarayana and Y. C. Shin, Two-photon lithography for three-dimensional fabrication in micro/nanoscale regime: A comprehensive review, *Opt. Laser Technol.*, 2021, **142**, 107180.
19 C. Greant, B. Van Durme, J. Van Hoorick and S. Van Vlierberghe, Multiphoton lithography as a promising tool for biomedical applications, *Adv. Funct. Mater.*, 2023, **33**(39), 2212641.
20 D. Yang, S. J. Jhaveri and C. K. Ober, Three-dimensional microfabrication by two-photon lithography, *MRS Bull.*, 2005, **30**(12), 976–982.
21 G. Zyla and M. Farsari, Frontiers of Laser–Based 3D Printing: A Perspective on Multi–Photon Lithography, *Laser Photonics Rev.*, 2024, **18**(7), 2301312.
22 P. Imrie and J. Jin, Polymer 4D printing: Advanced shape–change and beyond, *J. Polym. Sci.*, 2022, **60**(2), 149–174.
23 S. Feng, J. Cui, Y. Guo, W. Gao, Y. Sun, C. Liang, Z. Lu and B. Zhang, High performance and multi-UV curable materials adaptable photothermal nanoparticles for near-infrared-responsive digital light processing based 4D printing, *Compos. Sci. Technol.*, 2025, **260**, 110984.
24 X. Xia, J. Meng, J. Qin, G. Yang, P. Xuan, Y. Huang, W. Fan, Y. Gu, F. Lai and T. Liu, 4D-printed bionic soft robot with superior mechanical properties and fast near-infrared light response, *ACS Appl. Polym. Mater.*, 2024, **6**(6), 3170–3178.
25 P. Imrie and J. Jin, 4D Bioprinting: Keeping the Technology Alive, *Macromol. Mater. Eng.*, 2025, 2400386.
26 M. Chen, Y. Hou, R. An, H. J. Qi and K. Zhou, 4D printing of reprogrammable liquid crystal elastomers with synergistic photochromism and photoactuation, *Adv. Mater.*, 2024, **36**(34), 2303969.
27 S. Yu, N. Sadaba, E. Sanchez-Rexach, S. L. Hilburg, L. D. Pozzo, G. Altin-Yavuzarslan, L. M. Liz-Marzán, D. Jimenez de Aberasturi, H. Sardon and A. Nelson, 4D Printed Protein–AuNR Nanocomposites with Photothermal Shape Recovery, *Adv. Funct. Mater.*, 2024, **34**(14), 2311209.
28 J. Wang, X. Lin, R. Wang, Y. Lu and L. Zhang, Self–healing, photothermal–responsive, and shape memory polyurethanes for enhanced mechanical properties of 3D/4D printed objects, *Adv. Funct. Mater.*, 2023, **33**(15), 2211579.
29 A. H. Bonardi, F. Dumur, T. M. Grant, G. Noirbent, D. Gigmes, B. H. Lessard, J. P. Fouassier and J. Lalevée, High performance near-infrared (NIR) photoinitiating systems operating under low light intensity and in the presence of oxygen, *Macromolecules*, 2018, **51**(4), 1314–1324.
30 Z. Liu, T. Jia, Y. Yang, X. Yue, Y. Liu, X. Zhang, Y. Chen, S. Ma, C. Valenzuela, L. Wang and J. Shen, Near–infrared light–cured dental restoration materials with upconversion nanoparticles, *Chem. Eng. J.*, 2024, **488**, 150710.

31 A. H. Bonardi, F. Bonardi, F. Morlet-Savary, C. Dietlin, G. Noirbent, T. M. Grant, J. P. Fouassier, F. Dumur, B. H. Lessard, D. Gigmes and J. Lalevée, Photoinduced thermal polymerization reactions, *Macromolecules*, 2018, **51**(21), 8808–8820.
32 Z. Wu, K. Jung and C. Boyer, Effective Utilization of NIR Wavelengths for Photo–Controlled Polymerization: Penetration Through Thick Barriers and Parallel Solar Syntheses, *Angew. Chem., Int. Ed.*, 2020, **59**(5), 2013–2017.
33 Y. Zhao, J. Zhu, W. He, Y. Liu, X. Sang and R. Liu, 3D printing of unsupported multi-scale and large-span ceramic via near-infrared assisted direct ink writing, *Nat. Commun.*, 2023, **14**(1), 2381.
34 X. He, Y. Shao, Y. Xin, Y. Pang, Z. Jin, D. Guo and Y. Zou, Stereolithography 3D printing upon near-infrared photopolymerization, *Chem. Eng. J.*, 2025, 160857.
35 X. Zou, J. Zhu, Y. Zhu, Y. Yagci and R. Liu, Photopolymerization of macroscale black 3D objects using near-infrared photochemistry, *ACS Appl. Mater. Interfaces*, 2020, **12**(52), 58287–58294.
36 C. W. A. Bainbridge, M. Neradt, A. Avzalova, N. Broderick and J. Jin, Patterning of RAFT Polymer Networks by Laser Deactivation, *Macromol. Mater. Eng.*, 2024, **309**(5), 2300347.
37 H. I. Elim, B. Cai, O. Sugihara, T. Kaino and T. Adschiri, Rayleigh scattering study and particle density determination of a high refractive index TiO 2 nanohybrid polymer, *Phys. Chem. Chem. Phys.*, 2011, **13**(10), 4470–4475.
38 L. Wang, X. Yu, D. Zhang, Y. Wen, L. Zhang, Y. Xia, J. Chen, C. Xie, H. Zhu, J. Tong and Y. Shen, Long-term blue light exposure impairs mitochondrial dynamics in the retina in light-induced retinal degeneration in vivo and in vitro, *J. Photochem. Photobiol., B*, 2023, **240**, 112654.
39 L. A. Sordillo, S. Pratavieira, Y. Pu, K. Salas-Ramirez, L. Shi, L. Zhang, Y. Budansky and R. R. Alfano, Third therapeutic spectral window for deep tissue imaging, in *Optical biopsy XII*, SPIE, 2014, vol. 8940, pp. 128–134.
40 S. Wu and H. J. Butt, Near-infrared photochemistry at interfaces based on upconverting nanoparticles, *Phys. Chem. Chem. Phys.*, 2017, **19**(35), 23585–23596.
41 J. Zhu, Q. Zhang, T. Yang, Y. Liu and R. Liu, 3D printing of multi-scalable structures via high penetration near-infrared photopolymerization, *Nat. Commun.*, 2020, **11**(1), 3462.
42 J. Zhu, Z. Guo, Y. Zhou, X. Zou, Y. Zhu, Y. Liu and R. Liu, Chemical Optimization Strategy of Rapid Additive Manufacturing via Up–Conversion Assisted Photopolymerization Based Direct Ink Writing, *Adv. Mater. Technol.*, 2023, **8**(9), 2201613.
43 X. Zou, Y. Zhao, Y. Zhu and R. Liu, Filling aggregation-induced extinction mechanism in near-infrared photopolymerization for gradient and highly filled bulk materials, *Macromolecules*, 2022, **55**(6), 2075–2084.
44 Y. Zhao, G. Shi, J. T. Miao, X. Sang and R. Liu, Near-infrared photothermal dual crosslinking strategy for precise and efficient direct ink writing of high solids ceramic slurries, *Mater. Des.*, 2023, **235**, 112398.
45 W. Wu, H. Xu, J. T. Miao, X. Zou and R. Liu, Photothermal synergy mechanism in near-infrared photopolymerization for 3D printing acceleration and mechanical enhancement, *J. Mater. Chem. C*, 2024, **12**(34), 13379–13387.
46 C. Chen, X. Sang, D. Gao, Z. Zhu, W. Wu, Y. Zhao, J. T. Miao and R. Liu, Heterostructured Photoinitiator Comprising Upconversion Particles and Metal–Organic Frameworks for Enhanced Near-Infrared Photopolymerization: Implications for 3D Printing, *ACS Appl. Polym. Mater.*, 2024, **6**(18), 11557–11566.
47 Y. Chen, J. Zhang, X. Liu, S. Wang, J. Tao, Y. Huang, W. Wu, Y. Li, K. Zhou, X. Wei and S. Chen, Noninvasive in vivo 3D bioprinting, *Sci. Adv.*, 2020, **6**(23), eaba7406.
48 P. Zhang, Z. Teng, M. Zhou, X. Yu, H. Wen, J. Niu, Z. Liu, Z. Zhang, Y. Liu, J. Qiu and X. Xu, Upconversion 3D bioprinting for noninvasive in vivo molding, *Adv. Mater.*, 2024, **36**(14), 2310617.
49 D. A. Porter, N. Davis, P. S. Krueger, A. L. Cohen and D. Son, Additive manufacturing by material extrusion with medical grade silicone elastomers and IR laser curing, *Rapid Prototyp. J.*, 2020, **26**(1), 145–155.
50 V. V. Rocheva, A. V. Koroleva, A. G. Savelyev, K. V. Khaydukov, A. N. Generalova, A. V. Nechaev, A. E. Guller, V. A. Semchishen, B. N. Chichkov and E. V. Khaydukov, High-resolution 3D photopolymerization assisted by upconversion nanoparticles for rapid prototyping applications, *Sci. Rep.*, 2018, **8**(1), 3663.
51 A. Zhakeyev and J. Marques-Hueso, Centimeter-Scale Curing Depths in Laser-Assisted 3D Printing of Photopolymers Enabled by Er3+ Upconversion and Green Light-Absorbing Photosensitizer, *Photonics*, 2022, **9**(7), 498.
52 A. Zhakeyev, R. Devanathan and J. Marques-Hueso, Modification of a desktop FFF printer via NIR laser addition for upconversion 3D printing, *HardwareX*, 2024, **18**, e00520.
53 A. Zhakeyev, F. Walker, M. Abdulrhman and J. Marques-Hueso, Upconversion 3D printing enhancement via silver sensitization to enable selective metallization, *Opt. Mater.*, 2023, **142**, 114044.
54 A. Zhakeyev, M. Abdulrhman, Y. Zhang, F. Li, G. Chen and J. Marques-Hueso, Upconversion 3D printing enables single-immersion multi-material stereolithography, *Appl. Mater. Today*, 2023, **32**, 101854.
55 Q. Zhang, A. Boniface, V. K. Parashar, M. A. Gijs and C. Moser, Multi-photon polymerization using upconversion nanoparticles for tunable feature-size printing, *Nanophotonics*, 2023, **12**(8), 1527–1536.
56 L. M. Stevens, C. Tagnon and Z. A. Page, "Invisible" digital light processing 3D printing with near infrared light, *ACS Appl. Mater. Interfaces*, 2022, **14**(20), 22912–22920.
57 C. U. Lee, K. C. Chin and A. J. Boydston, Additive manufacturing by heating at a patterned photothermal interface, *ACS Appl. Mater. Interfaces*, 2023, **15**(12), 16072–16078.

58 D. Kam, O. Rulf, A. Reisinger, R. Lieberman and S. Magdassi, 3D printing by stereolithography using thermal initiators, *Nat. Commun.*, 2024, **15**(1), 2285.
59 P. Acosta-Mora, K. Domen, T. Hisatomi, H. Lyu, J. Méndez-Ramos, J. C. Ruiz-Morales and N. M. Khaidukov, Shifting the NIR into the UV-blue: Up-conversion boosted photocatalysis, *Opt. Mater.*, 2018, **83**, 315–320.
60 Z. Chen, X. Wang, S. Li, S. Liu, H. Miao and S. Wu, Near–Infrared Light Driven Photopolymerization Based On Photon Upconversion, *ChemPhotoChem*, 2019, **3**(11), 1077–1083.
61 Z. Chen, S. He, H. J. Butt and S. Wu, Photon upconversion lithography: patterning of biomaterials using near-infrared light, *Adv. Mater.*, 2015, **27**(13), 2203–2206.
62 G. Chen, H. Qiu, P. N. Prasad and X. Chen, Upconversion nanoparticles: design, nanochemistry, and applications in theranostics, *Chem. Rev.*, 2014, **114**(10), 5161–5214.
63 J. Méndez-Ramos, J. C. Ruiz-Morales, P. Acosta-Mora and N. M. Khaidukov, Infrared-light induced curing of photosensitive resins through photon up-conversion for novel cost-effective luminescent 3D-printing technology, *J. Mater. Chem. C*, 2016, **4**(4), 801–806.
64 M. Yan, L. Guo, P. Cai, Y. Huang, Q. Zhang and Q. Lue, Hydrothermal synthesis of NaYF4: Yb3+, Tm3+ upconversion microparticles and their effects on polymerization for stereolithography, *Opt. Mater.*, 2020, **109**, 110311.
65 J. Hodak, Z. Chen, S. Wu and R. Etchenique, Multiphoton excitation of upconverting nanoparticles in pulsed regime, *Anal. Chem.*, 2016, **88**(2), 1468–1475.
66 L. Rodríguez-Pombo, L. Martínez-Castro, X. Xu, J. J. Ong, C. Rial, D. N. García, A. González-Santos, J. Flores-González, C. Alvarez-Lorenzo, A. W. Basit and A. Goyanes, Simultaneous fabrication of multiple tablets within seconds using tomographic volumetric 3D printing, *Int. J. Pharm.:X*, 2023, **5**, 100166.
67 W. Liang, D. Xiao, W. Zhang, Y. Ni, H. Wan, X. Xu, S. Zhang and S. Ruan, Infrared light induced deep ultraviolet internal light centers for novel cost-effective 3D printing, *J. Alloys Compd.*, 2021, **863**, 158053.
68 Q. Thijssen, J. Toombs, C. C. Li, H. Taylor and S. Van Vlierberghe, From pixels to voxels: a mechanistic perspective on volumetric 3D-printing, *Prog. Polym. Sci.*, 2023, **147**, 101755.
69 E. Shang, G. Li, Z. Zhao, N. Zhang, D. Fan and Y. Liu, Laser–assisted direct ink writing for high–fidelity fabrication of elastomeric complex structures, *Adv. Mater. Interfaces*, 2023, **10**(28), 2300300.
70 D. W. Yee, A HAPPI solution: Photothermal additive manufacturing of unmodified thermoset resins, *Matter*, 2023, **6**(8), 2599–2601.
71 D. Kam, R. Lieberman, N. Trink, O. Rulf and S. Magdassi, Vat photopolymerization printing by thermal polymerisation utilising carbon nanotubes as photothermal converters, *Virtual Phys. Prototyping*, 2024, **19**(1), e2391480.
72 K. Sun, X. Peng, Z. Gan, W. Chen, X. Li, T. Gong and P. Xiao, 3D printing/vat photopolymerization of photopolymers activated by novel organic dyes as photoinitiators, *Catalysts*, 2022, **12**(10), 1272.
73 J. P. Goddard, N. Sellet, J. Frey and M. Cormier, Near-infrared photocatalysis with cyanines: synthesis, applications and perspectives, *Chem. Sci.*, 2024, **15**(23), 8639–8650.
74 L. M. Stevens, N. T. Almada, H. S. Kim and Z. A. Page, Visible-Light-Fueled Polymerizations for 3D Printing, *Acc. Chem. Res.*, 2025, **58**(2), 250–260.
75 S. Allison-Logan, Q. Fu, Y. Sun, M. Liu, J. Xie, J. Tang and G. G. Qiao, From UV to NIR: A Full–Spectrum Metal–Free Photocatalyst for Efficient Polymer Synthesis in Aqueous Conditions, *Angew. Chem.*, 2020, **132**(48), 21576–21580.
76 V. Ferraro, C. R. Adam, A. Vranic and S. Bräse, Recent advances of transition metal complexes for photopolymerization and 3D printing under visible light, *Adv. Funct. Mater.*, 2024, **34**(20), 2302157.
77 A. Stafford, S. R. Allen, T. A. Grusenmeyer, C. J. O'Dea, L. Estergreen, S. T. Roberts and Z. A. Page, Thiophene-fused boron dipyrromethenes as energy efficient near-infrared photocatalysts for radical polymerizations, *J. Mater. Chem. A*, 2023, **11**(41), 22259–22266.
78 A. Stafford, S. R. Allen, L. Estergreen, K. Kafle, S. T. Roberts and Z. A. Page, Efficient near-infrared photopolymerizations using azaBODIPYs with electron-donating groups and intramolecular charge transfer, *Macromolecules*, 2023, **56**(23), 9804–9810.
79 P. Imrie, O. Diegel and J. Jin, Direct-ink-write 3D printing of "living" polymer hydrogels via type I photoinitiated RAFT polymerization, *Polymer*, 2023, **276**, 125944.
80 P. Imrie and J. Jin, Gelation of RAFT polymer networks analyzed by rheology, *Polymer*, 2025, **317**, 127956.
81 A. Bagheri, Application of RAFT in 3D printing: where are the future opportunities?, *Macromolecules*, 2023, **56**(5), 1778–1797.
82 P. Imrie and J. Jin, Mechanical Property Modification of "Living" Networks via PET–RAFT Photopolymerization, *Macromol. Symp.*, 2023, **408**(1), 2100506.
83 M. Asadi-Eydivand, T. C. Brown and A. Bagheri, RAFT-mediated 3D printing of "living" materials with tailored hierarchical porosity, *ACS Appl. Polym. Mater.*, 2022, **4**(7), 4940–4948.
84 J. Li, M. Chen, X. Lin, Q. Li, W. Zhang, G. Jin, X. Pan, J. Zhu and X. Zhu, Near-infrared, light-induced cationic and radical RAFT polymerization catalyzed by iron complex, *ACS Macro Lett.*, 2020, **9**(12), 1799–1805.
85 B. Zhao, J. Li, X. Pan, Z. Zhang, G. Jin and J. Zhu, Photoinduced free radical promoted cationic RAFT polymerization toward "living" 3D printing, *ACS Macro Lett.*, 2021, **10**(10), 1315–1320.
86 X. D. Su, Q. Liu, J. T. Cheng, Z. X. Wang and X. Y. Chen, Near-Infrared-Light-Induced Iron(I) Dimer-Enabled Radical Cascade Reactions of Fluoroalkyl Bromides for the Synthesis of Ring-Fused Quinazolinones, *Org. Lett.*, 2024, **26**(37), 7976–7980.
87 X. D. Su, Q. Liu, X. N. Li, B. B. Zhang, Z. X. Wang and X. Y. Chen, Near-infrared-light-induced iron(I) dimer-

enabled halogen atom transfer for rapid iodoperfluoroalkylation of alkenes, *Chem. Catal.*, 2023, **3**(8), 100710.

88 S. He, Y. Zhu, Y. Lu, Z. Shi, Y. Wang, J. Li, J. Zhu and N. Li, Metal-Free Near-Infrared-Induced Radical-Promoted Cationic RAFT Polymerization for High Penetration Photocuring, *Polym. Chem.*, 2025, **16**(14), 1613–1618.

89 L. Huang, L. Zeng, Y. Chen, N. Yu, L. Wang, K. Huang, Y. Zhao and G. Han, Long wavelength single photon like driven photolysis via triplet triplet annihilation, *Nat. Commun.*, 2021, **12**(1), 122.

90 S. N. Sanders, T. H. Schloemer, M. K. Gangishetty, D. Anderson, M. Seitz, A. O. Gallegos, R. C. Stokes and D. N. Congreve, Triplet fusion upconversion nanocapsules for volumetric 3D printing, *Nature*, 2022, **604**(7906), 474–478.

91 D. K. Limberg, J. H. Kang and R. C. Hayward, Triplet–triplet annihilation photopolymerization for high-resolution 3D printing, *J. Am. Chem. Soc.*, 2022, **144**(12), 5226–5232.

92 J. M. Park, H. Lee, H. S. Choe, S. K. Ahn, K. Y. Seong, S. Y. Yang and J. H. Kim, Highly efficient triplet–triplet annihilation upconversion in polycaprolactone: application to 3D printable architectures and microneedles, *J. Mater. Chem. C*, 2022, **10**(12), 4584–4589.

93 J. Wong, S. Wei, R. Meir, N. Sadaba, N. A. Ballinger, E. K. Harmon, X. Gao, G. Altin-Yavuzarslan, L. D. Pozzo, L. M. Campos and A. Nelson, Triplet Fusion Upconversion for Photocuring 3D–Printed Particle–Reinforced Composite Networks, *Adv. Mater.*, 2023, **35**(11), 2207673.

94 Z. Luo, D. Wang, K. Li, D. Zhong, L. Xue, Z. Gan and C. Xie, Three-dimensional nanolithography with visible continuous wave laser through triplet up-conversion, *J. Phys. Chem. Lett.*, 2023, **14**(3), 709–715.

95 Z. Wang, Y. Zhang, Y. Su, C. Zhang and C. Wang, Three-dimensional direct-writing via photopolymerization based on triplet—triplet annihilation, *Sci. China: Chem.*, 2022, **65**(11), 2283–2289.

96 C. J. O'Dea, J. Isokuortti, E. E. Comer, S. T. Roberts and Z. A. Page, Triplet upconversion under ambient conditions enables digital light processing 3D printing, *ACS Cent. Sci.*, 2024, **10**(2), 272–282.

97 A. Caron, G. Noirbent, D. Gigmes, F. Dumur and J. Lalevée, Near–Infrared PhotoInitiating Systems: Photothermal versus Triplet–Triplet Annihilation–Based Upconversion Polymerization, *Macromol. Rapid Commun.*, 2021, **42**(11), 2100047.

98 L. Huang and G. Han, Triplet–triplet annihilation photon upconversion-mediated photochemical reactions, *Nat. Rev. Chem.*, 2024, **8**(4), 238–255.

99 Y. Peng, J. Y. Li, F. Qi, D. X. Guo, Y. Z. Li, H. J. Feng, L. H. Jiang, M. Y. Zhang, Y. X. Liu, L. Zeng and L. Huang, Highly Effective Near-Infrared to Blue Triplet–Triplet Annihilation Upconversion Nanoparticles for Reversible Photobiocatalysis, *Nano Lett.*, 2025, **25**(13), 5291–5298.

100 Y. Qi, H. Lv, Q. Huang and G. Pan, Employing a combination of direct ink writing and near-infrared-induced photopolymerization facilitates 3D printing of unsupported multi-scale ceramics: The bone tissue engineering approach, *Eur. Polym. J.*, 2024, 113133.

101 Y. Fang, Y. Guo, T. Liu, R. Xu, S. Mao, X. Mo, T. Zhang, L. Ouyang, Z. Xiong and W. Sun, Advances in 3D bioprinting, *Chin. J. Mech. Eng.*, 2022, **1**(1), 100011.

102 X. Wang, Bioartificial organ manufacturing technologies, *Cell Transplant.*, 2019, **28**(1), 5–17.

103 H. Goodarzi Hosseinabadi, E. Dogan, A. K. Miri and L. Ionov, Digital light processing bioprinting advances for microtissue models, *ACS Biomater. Sci. Eng.*, 2022, **8**(4), 1381–1395.

104 J. Liu, B. Zhang, Z. Lu, J. W. Shen, P. Zhang and Y. Yu, Interfacial Engineering of High-Performance Upconversion Hydrogels with Orthogonal NIR Photochemistry in Vivo for Synergistic Noninvasive Biofilm Elimination and Tissue Repair, *Chem. Mater.*, 2024, **36**(12), 6276–6287.

105 P. Karami, V. K. Rana, Q. Zhang, A. Boniface, Y. Guo, C. Moser and D. P. Pioletti, NIR light-mediated photocuring of adhesive hydrogels for noninvasive tissue repair via upconversion optogenesis, *Biomacromolecules*, 2022, **23**(12), 5007–5017.

106 Z. Chen, W. Sun, H. J. Butt and S. Wu, Upconverting–Nanoparticle–Assisted Photochemistry Induced by Low–Intensity Near–Infrared Light: How Low Can We Go?, *Chem. – Eur. J.*, 2015, **21**(25), 9165–9170.

107 B. E. Kelly, I. Bhattacharya, H. Heidari, M. Shusteff, C. M. Spadaccini and H. K. Taylor, Volumetric additive manufacturing via tomographic reconstruction, *Science*, 2019, **363**(6431), 1075–1079.

108 M. Kollep, G. Konstantinou, J. Madrid-Wolff, A. Boniface, L. Hagelüken, P. V. W. Sasikumar, G. Blugan, P. Delrot, D. Loterie, J. Brugger and C. Moser, Tomographic volumetric additive manufacturing of silicon oxycarbide ceramics, *Adv. Eng. Mater.*, 2022, **24**(7), 2101345.

109 M. Regehly, Y. Garmshausen, M. Reuter, N. F. König, E. Israel, D. P. Kelly, C. Y. Chou, K. Koch, B. Asfari and S. Hecht, Xolography for linear volumetric 3D printing, *Nature*, 2020, **588**(7839), 620–624.

110 N. F. König, M. Reuter, M. Reuß, C. S. F. Kromer, M. Herder, Y. Garmshausen, B. Asfari, E. Israel, L. Vasconcelos Lima, N. Puvati and J. Leonhard, Xolography for 3D Printing in Microgravity, *Adv. Mater.*, 2025, **37**(5), 2413391.

111 D. Loterie, P. Delrot and C. Moser, High-resolution tomographic volumetric additive manufacturing, *Nat. Commun.*, 2020, **11**(1), 852.

112 L. Stüwe, M. Geiger, F. Röllgen, T. Heinze, M. Reuter, M. Wessling, S. Hecht and J. Linkhorst, Continuous volumetric 3D printing: xolography in flow, *Adv. Mater.*, 2024, **36**(4), 2306716.

113 L. Wei, C. Yang and W. Wu, Recent advances of stereolithographic 3D printing enabled by photon upconversion technology, *Curr. Opin. Green Sustain. Chem.*, 2023, **43**, 100851.

114 L. Rodríguez-Pombo, X. Xu, A. Seijo-Rabina, J. J. Ong, C. Alvarez-Lorenzo, C. Rial, D. Nieto, S. Gaisford, A. W. Basit and A. Goyanes, Volumetric 3D printing for rapid production of medicines, *Addit. Manuf.*, 2022, **52**, 102673.

115 A. Fernandez-Bravo, D. Wang, E. S. Barnard, A. Teitelboim, C. Tajon, J. Guan, G. C. Schatz, B. E. Cohen, E. M. Chan, P. J. Schuck and T. W. Odom, Ultralow-threshold, continuous-wave upconverting lasing from subwavelength plasmons, *Nat. Mater.*, 2019, **18**(11), 1172–1176.

116 S. Zhu, L. Wei, Y. Sun, C. Yang and W. Wu, NIR/Visible Light Double Beam Synergistically Enhanced the Emission of Triplet–Triplet Annihilation Upconversion via Thermal Lensing Effect, *Adv. Opt. Mater.*, 2023, **11**(18), 2300484.

117 P. Chansoria, D. Rütsche, A. Wang, H. Liu, D. D'Angella, R. Rizzo, A. Hasenauer, P. Weber, W. Qiu, N. B. M. Ibrahim and N. Korshunova, Synergizing algorithmic design, photoclick chemistry and multi–material volumetric printing for accelerating complex shape engineering, *Adv. Sci.*, 2023, **10**(26), 2300912.